

https://doi.org/10.1070/QEL17312

Effect of optical field ionisation on the generation of wake fields by femtosecond laser pulses in an inhomogeneous plasma

I.R. Umarov, N.E. Andreev

Abstract. **We consider the interaction of a high-intensity short laser pulse with an argon gas during optical field ionisation. Modelling in a three-dimensional cylindrical symmetric geometry is performed at various moderately relativistic intensities and positions of the focal plane of the laser beam in the case of both optical gas ionisation and a pre-ionised plasma. The influence of the processes occurring during optical field ionisation of the gas on the generation of wake waves is investigated, and the conditions are found under which intense wake fields are produced in a plasma formed from an inhomogeneous argon gas jet. The possibility of using a gas with a large number of electrons on the outer shell (argon) to excite intense wake waves and accelerate electrons is demonstrated. Despite significant ionisation refraction of the laser pulse on a radially inhomogeneous density profile of plasma electrons formed during optical field ionisation, the region of the parameters of the laser pulse and the gas target is determined at which ionisation refraction leads to the excitation of an intense wake wave. It is found that in a pre-ionised plasma a wake wave is not generated even at the same laser radiation intensity.**

Keywords: *wake fields, femtosecond laser pulses, inhomogeneous plasma.*

1. Introduction

Presently, many research programmes include laser-plasma acceleration of particles. At the current level of development, electron beams with energies of GeV or higher have already been obtained. For example, the possibility of electron acceleration in the field of a wake wave to energies of ~8 GeV at relatively small (~10 cm) distances was experimentally demonstrated by Gonsalves et al. [1].

The processes occurring during optical field ionisation of a gas by a laser pulse can play a dramatic role in laser-plasma interaction. Thus, Emenko et al. [2] studied various processes, including the appearance of large and small structures in a plasma. Andreev et al. [3, 4] showed that optical field ionisation can significantly increase the amplitude of the excited wake wave in the case when the laser pulse is longer than the plasma wavelength. In some cases, ionisation can give rise to the laser pulse self-modulation [5] at such parameters of the problem when this self-modulation is impossible without ionisation [4]. Other important processes include ionisation refraction. Thus, Leemans et al. [6] examined the dependence of ionisation refraction on the gas density, and Andreev et al. [7] analysed how the number of electrons on the outer shell of the atom affect ionisation refraction. They found that when use is made of a gas with a large number of electrons on the outer shell, ionisation refraction leads to significant changes in the shape of the laser pulse and to a decrease in its intensity. However, atoms with a large number of electrons on the outer shell are used in schemes with ionisation injection, when electrons are captured from the inner shells. Therefore, in many experiments, for example, in [8], ionisation refraction with a small admixture of atoms with a large number of electrons on the outer shell (argon) necessary for ionisation injection is reduced by employing a plasma of elements with a small number of valence electrons (hydrogen). Another way to reduce the effect of ionisation refraction is to use pre-formed plasma channels without impurities, as, for example, in [9], where ionisation trapping of electrons was demonstrated in a nitrogen plasma.

The aim of this work, unlike the ones mentioned above, is to consider the effect of optical field ionisation on laser-plasma interaction and generation of wake waves in a plasma of elements with a high atomic number without using impurities and pre-formed channels. As an example, we use an argon gas jet at various parameters of the laser pulse.

2. Equations of the model

To describe the dynamics of the interaction of a laser pulse with plasma electrons emerging during optical field ionisation of the gas, we used the hydrodynamic model of a cold plasma and Maxwell's equations, which in the case of cylindrical symmetry can be written as [10, 11]

$$\left[2\mathrm{i}\frac{\partial}{\partial\zeta}+\frac{k_{\mathrm{p0}}}{k_0}\left(\Delta_{\perp\rho}+\frac{\partial^2}{\partial\zeta\partial\xi}\right)\right]a=\frac{k_{\mathrm{p0}}}{k_0}\left[\frac{\nu}{\gamma}a-\mathrm{i}G_{\mathrm{ion}}\right], \tag{1}$$

$$\left[(\Delta_{\perp\rho}-\nu_0)\frac{\partial^2}{\partial\xi^2}-\frac{\partial\ln\nu_0}{\partial\rho}\frac{\partial^3}{\partial\rho\partial\xi^2}+\nu_0\Delta_{\perp\rho}\right]\Phi$$
$$-\frac{\nu_0^2}{2}\left[1-\frac{1+|a|^2/2}{(\Phi+\delta\Phi_{\mathrm{s}})^2}\right]=\frac{\nu_0}{4}\Delta_{\perp\rho}|a|^2, \tag{2}$$

I.R. Umarov, N.E. Andreev Moscow Institute of Physics and Technology (National Research University), Institutskii per. 9, 141701 Dolgoprudnyi, Moscow region, Russia; Joint Institute for High Temperatures, Russian Academy of Sciences, ul. Izhorskaya 13/2, 125412 Moscow, Russia; e-mail: iskan1997@yandex.ru

Received 4 March 2020; revision received 30 April 2020
Kvantovaya Elektronika **50** (8) 770–775 (2020)
Translated by I.A. Ulitkin

$$\frac{\nu}{\gamma} = \frac{\nu_0 + \Delta_{\perp\rho}\Phi}{\Phi + \delta\Phi_s}, \tag{3}$$

where $\Delta_{\perp\rho}$ is the radial component of the Laplacian; a is the dimensionless envelope of the electric field of the laser pulse:

$$\frac{\epsilon \boldsymbol{E}}{m\omega_0 c} = \mathrm{Re}[\boldsymbol{\epsilon}_0 a \exp(-\mathrm{i}\omega_0 t + \mathrm{i}k_0 z)]; \tag{4}$$

$\boldsymbol{\epsilon}_0$ is the unit polarisation vector perpendicular to the z axis [7] (the laser pulse is assumed to be linearly polarised); ω_0 is the laser pulse frequency; and $k_0 = \omega_0/c$ is the modulus of its wave vector. Equation (1) describes the change in the laser pulse envelope, equation (2) determines the potential of the wake field Φ ($\delta\Phi_s$ is the contribution of the optical field ionisation to the wake potential), and equation (3) relates the value of the potential to the electron density: $\nu = n/N_0$ is the electron density normalised to a constant value N_0; $\nu_0 = n_0/N_0$ is the normalised unperturbed density of electrons formed during optical field ionisation by a laser pulse (for more details, see [11, 12]). In these equations, use is made of the dimensionless variables accompanying the laser pulse:

$$\xi = k_{p0}(z - ct), \quad \zeta = k_{p0}z, \quad \rho = k_{p0}r_\perp, \tag{5}$$

where $k_{p0} = \omega_{p0}/c = (4\pi e^2 N_0/m)^{1/2}/c$ is the modulus of the plasma wave vector. The relativistic gamma factor of electrons averaged over fast oscillations in the electric field of a laser pulse is $\gamma = [1 + |\boldsymbol{q}|^2 + |a|^2/2]^{1/2}$, where $\boldsymbol{q} = \boldsymbol{p}/(mc)$ is the dimensionless momentum of plasma electrons due to motion in wake fields. The energy loss of a laser pulse due to ionisation is described in equation (1) by the dimensionless ionisation current G_{ion}. In equations (1)–(3), the small longitudinal component of the electric field E_z of the laser pulse is neglected [due to the smallness of the parameter $(k_0 r_0)^{-1}$], where r_0 is the radius of the laser pulse spot in the focal plane).

The unperturbed electron density n_0 and the ionisation current G_{ion} arising in the process of gas ionisation by a laser pulse are determined by the ionisation kinetics equations for the ion densities $\bar{N}_k$ with the degree of ionisation k ($k = 0, 1, \ldots, Z_n$, where Z_n is the nuclear charge). The electron production rate averaged over the laser pulse period is expressed as

$$\Gamma_0 = \frac{\partial n_0}{\partial t} \equiv \sum_{k=1}^{Z_n} k\frac{\partial \bar{N}_k}{\partial t} = \sum_{k=0}^{Z_n-1} \bar{W}_k \bar{N}_k \equiv \sum_{k=0}^{Z_n-1} \Gamma_0^{(k)}. \tag{6}$$

This rate is determined by the Ammosov–Delone–Krainov formula $\bar{W}_k(|\boldsymbol{E}|)$ averaged over the laser pulse period [13, 14] (see also [15]), where $|\boldsymbol{E}|$ is the electric field envelope of the laser pulse, defined by equation (1).

The equations describing the ionisation process and averaged over the period of laser radiation can be written as

$$\frac{\partial D_0}{\partial t} = -\bar{W}_0 D_0, \tag{7}$$

$$\frac{\partial D_k}{\partial t} = (\bar{W}_{k-1} D_{k-1} - \bar{W}_k D_k), \quad k = 1, 2, \ldots, Z_{n-1}, \tag{8}$$

where $D_k = \bar{N}_k/n_a$ are the ion densities with degrees of ionisation k, normalised to the time-independent gas density

$$n_a(\boldsymbol{r}) = \sum_{k=0}^{Z_n} N_k.$$

The solution to equations (7) and (8) allows us to determine the electron density n_0 unperturbed by wake and laser fields, arising from optical field ionisation, as well as the electron production rate Γ_0:

$$n_0 = n_a\left[(1 - D_0)Z_n - \sum_{k=1}^{Z_n-1}(Z_n + 1 - k)D_k\right], \tag{9}$$

$$\Gamma_0 = n_a \sum_{k=0}^{Z_n-1} \bar{W}_k D_k \equiv \sum_{k=0}^{Z_n-1} \Gamma_0^{(k)}. \tag{10}$$

Equation (9) is the law of conservation of charge

$$n_0 = n_a \sum_{k=1}^{Z_n} k D_k$$

with the substitution

$$D_{Z_n} = 1 - \sum_{k=0}^{Z_n-1} D_k,$$

making it possible not to solve the equation for D_{Z_n}. Equation (10) is equation (6) written in terms of normalised densities of ions D_k, for which equations (7) and (8) were solved. Spatial and temporal dependences of the normalised ion densities $D_k(r_\perp, z, t)$ determine the ionisation state of the corresponding ion irrespective of the inhomogeneous density of atoms and allow the average multiplicity of gas ionisation to be defined

$$\alpha(r_\perp, z, t) = \sum_{k=1}^{Z_n} k D_k(r_\perp, z, t). \tag{11}$$

The distributions of the maximum average degree of ionisation on the laser pulse axis, $\alpha_{max} = \alpha(r_\perp = 0, z, t \to \infty)$, are shown below in Figs 3–7.

In this case, the dimensionless ionisation current G_{ion} can be expressed in terms of the electron production rate:

$$G_{ion} = \frac{4\pi e}{m\omega_{p0}^2 c} J_{ion} = \frac{k_{p0}}{k_0}\left[\frac{2a}{|a|^2}\sum_{k=0}^{Z_n-1} S_0^{(k)} \frac{U_k}{mc^2} - \frac{a^* S_2}{4}\right], \tag{12}$$

where

$$S_0^{(k)} = \frac{\Gamma_0^{(k)}}{N_0 \omega_{p0}}; \quad S_2 \approx 2\mu \sum_{k=0}^{Z_n-1} S_0^{(k)}$$

is the normalised second harmonic of the electron production rate [16], and U_k is the ionisation energy of the kth electron.

3. Calculation parameters

We performed a series of calculations in the range of peak laser intensities of $(0.7–1.3) \times 10^{18}$ W cm^{-2}, which corresponds to the range of peak laser pulse powers of 71–133 GW, to the range of laser pulse energies of 71–133 mJ, and to the dimensionless field amplitude a_0 in the range of 0.57–0.78. A linearly polarised laser pulse with a wavelength $\lambda_0 = 0.8$ μm had a Gaussian envelope in time and a Gaussian radial profile (Fig. 1):

$$a(\xi, \rho) = a_0 \exp\left[-2\ln 2\frac{(\xi - \xi_0)^2}{\omega_{p0}^2 t_{imp}^2} - \frac{\rho^2}{k_{p0}^2 r_0^2}\right], \tag{13}$$

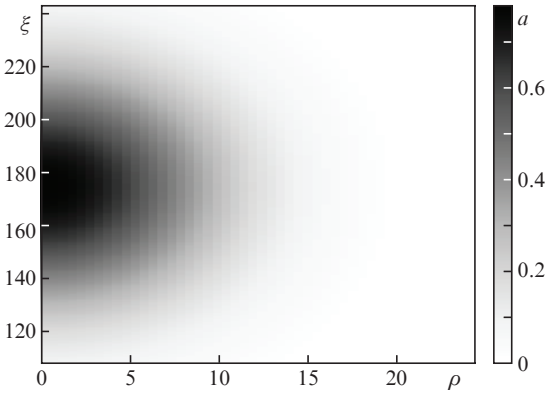

Figure 1. Spatial distribution of the field amplitude a in the focal plane; $z = 0$.

where $t_{imp} = 47.3$ fs is the laser pulse duration (full width at half maximum of intensity); $r_0 = 2.55$ μm is the radius of the spot in the focal plane; and ξ_0 is the position of the maximum.

We considered the interaction of laser radiation with an inhomogeneous argon gas profile with a maximum density of 4.98×10^{19} cm^{-3} (Fig. 2):

$$n_a = \begin{cases} n_0 \exp[-(z_{min} - z)^2/D^2], & z < z_{min}, \\ n_0, & z_{min} \leqslant z \leqslant z_{max}, \\ n_0 \exp[-(z - z_{max})^2/D^2], & z > z_{max}, \end{cases} \quad (14)$$

where $z_{min} = 270$ μm, $z_{max} = 770$ μm, $D = 150$ μm, and $n_0 = 4.98 \times 10^{19}$ cm^{-3}.

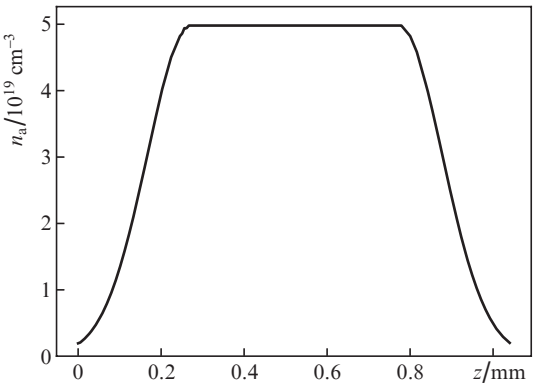

Figure 2. Normalised spatial distribution of the density of argon atoms.

The calculations were performed for different conditions for laser pulse focusing, namely, at different positions of the focal plane relative to the beginning of the calculation domain, as well as with allowance for ionisation and in a preliminarily eightfold ionised argon plasma. We used the LAser-PLasma ACceleration (LAPLAC) code [17], modified to take into account optical field ionisation [11] and based on the grid method. In our calculations, we used a grid of size 0.05 in ξ, 0.02 in ρ, and 20 in ζ.

For convenience, we present the values of some dimensionless quantities. The electron density was normalised to $N_0 = 3.99 \times 10^{20}$ cm^{-3}, representing the atom density multiplied by eight, which corresponds to the electron density on the plateau during eightfold ionisation that was found in the region of interest to us. The spatial parameters (ξ, ζ, ρ) are measured in units of $k_{p0}^{-1} \approx 0.267$ μm. The electric field amplitude of the laser pulse is represented by the dimensionless quantity a, and $a = 1$ approximately corresponds to $E \approx 4.01 \times 10^9$ V m^{-1}.

4. Simulation results

First, we consider a pulse with a peak intensity of 1.3×10^{18} W cm^{-2} focused at the beginning of the calculation domain (focal plane $z = 0$). Let us compare the cases of optical field ionisation of the gas by a laser pulse and the choice of a plasma of preliminarily eightfold ionised argon (Fig. 3).

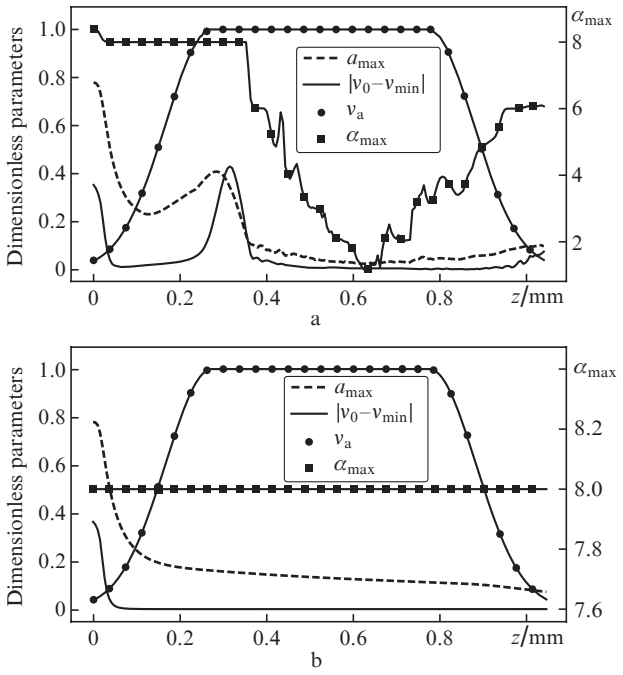

Figure 3. Distributions of the maximum dimensionless amplitude of the laser pulse field (a_{max}), the maximum amplitude of the wake wave ($|v_0 - v_{min}|$), the maximum degree of ionisation (α_{max}) and the normalised gas concentration (v_a) on the laser pulse propagation axis in the cases of (a) optical field ionisation and (b) a pre-ionised plasma.

One can see that at the beginning of the calculation domain of the region ($z < 0.1$ mm), where the gas density and, accordingly, the density of plasma electrons are small, the dynamics of parameters (such as the laser pulse amplitude and electron density) characterising laser pulses and plasma are almost identical. However, it is seen that in the case of optical field ionisation, the laser pulse amplitude ceases to fall and begins to grow already at a distance of 0.1 mm. This is due to the fact that in the case of optical field ionisation, a wake wave begins to be generated, while this does not occur in a pre-ionised plasma at the same parameters. The generation of the wake wave in the case of optical field ionisation stems from the scattering of part of the energy due to stronger refraction of the laser pulse front, associated with the inhomogeneity of the electron density profile, as well as with ionisation losses at the leading edge of the laser pulse. Therefore, the laser pulse in the case of optical field ionisation acquires a very sharp front, which contributes to the initial generation of the wake wave (Fig. 4).

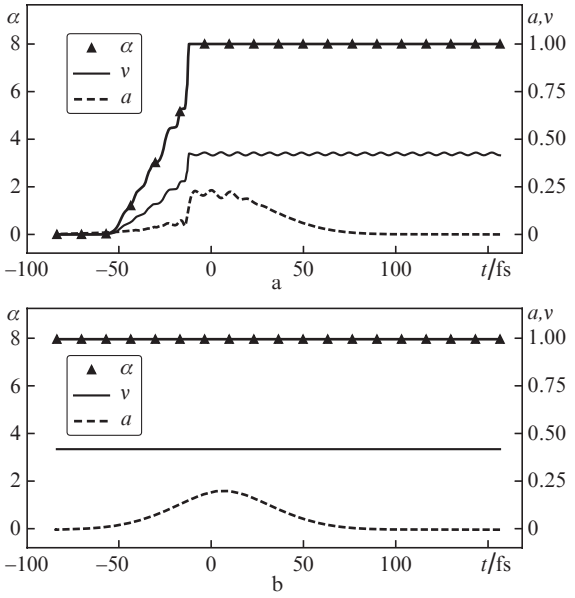

Figure 4. Comparison of the time dependences of the laser pulse envelopes (a), electron densities (v), and degrees of ionisation (α) on the laser beam axis in the cases of (a) optical field ionisation and (b) a pre-ionised plasma at point $\zeta = 500$ ($z = 133.4$ μm). In the case of optical field ionisation, a sharp laser front is clearly visible near the –15 fs point, which contributes to the emergence of a wake wave; $t = 0$ corresponds to the position in which the maximum amplitude of the laser pulse would be located during propagation in a vacuum.

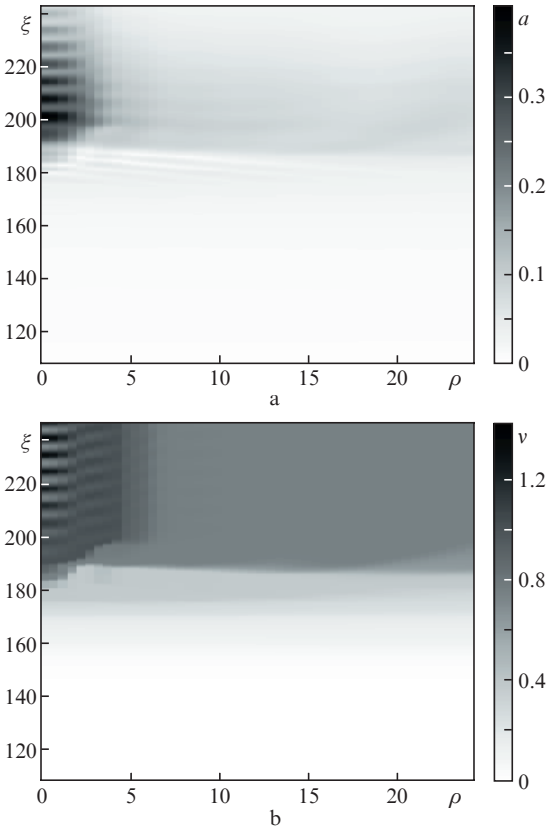

Figure 5. Two-dimensional distributions of (a) laser pulse amplitude $a(\xi,\rho)$ and (b) electron density $v(\xi,\rho)$ at point $\zeta = 1100$ ($z = 293.5$ μm). The zones of increased and decreased electron densities on the axis and the corresponding zones of the laser pulse amplitude are clearly visible.

One can also see the onset of self-modulation and, accordingly, self-focusing of the laser pulse in the generated wake wave, which contributes to a further increase in its amplitude. We stipulate in advance that in most subsequent cases, self-focusing, if present, is simultaneously the result of both mechanisms, i.e. relativistic and ponderomotive (their influence in the case of simultaneous presence was discussed in more detail in [18]), except for the only case that will be discussed separately. The resulting configurations of the wake field and laser pulse are presented in more detail in Fig. 5. One can see that the edges of the wake wave slightly lag behind its centre, which produced alternating zones of increased and decreased electron density on the laser pulse propagation axis relative to the electron density at some distance from the axis; this leads to the observed phenomena of the laser pulse self-focusing and self-modulation.

The desired intensity of the laser pulse can be reduced if it is focused not into the beginning of the calculation domain, but into the gas. Thus, it is possible to obtain similar results, but at half the intensity when the pulse is focused at a distance $\zeta = 300$ ($z = 0.08$ mm) (Fig. 6a). In the same way, a pulse with an intensity of 1.0×10^{18} W cm^{-2} was focused in the absence of optical ionisation in a pre-ionised plasma (Fig. 6b).

Although we obtain an intensity sufficient for relativistic self-focusing in a pre-ionised plasma (Fig. 6b), excitation of wake waves still does not occur – this indicates the key role of the processes that occur during optical field ionisation (in particular, a change in the laser pulse shape) – in the case of excitation of the wake wave in a preliminary unionised plasma. A direct comparison of all four cases at point $\zeta = 1200$ ($z = 330.4$ μm) is shown in Fig. 7. One can clearly see that in the case of focusing into the gas, the wake wave has a larger amplitude even at half the intensity, while in the cases of a pre-ionised plasma, there are at least no noticeable perturbations of the electron density at the same and even higher intensities, except for the regions near the focal planes of the laser pulse. In these cases, the electron density changes as a result of the displacement of electrons from the axis by the ponderomotive forces of the laser pulse without excitation of wake waves.

One of the main differences between a pre-ionised plasma and a plasma obtained during optical field ionisation in the case of a gas of relatively heavy atoms is the formation of an inhomogeneous plasma profile with a maximum on the axis of the laser pulse propagation, resulting in an inhomogeneous distribution of the refractive index with a maximum on the axis, which contributes to much faster refraction of the laser pulse. It is this fact that is the main limitation in the case of optical field ionisation in terms of choosing the focusing distance: At sufficiently large distances, the laser beam begins to diverge due to refraction on an inhomogeneous electron density until it reaches its focal plane. For this reason, the laser pulses were focused relatively shallowly, to a distance of $\zeta \approx 300$ ($z = 80$ μm). As an example, Fig. 8 compares the dynamics of the amplitudes of laser pulses (with initially specified peak intensities in the focal plane, which, when propagate in a vacuum, are 0.7×10^{18} W cm^{-2}) in cases of focusing at distances from $\zeta = 250$ ($z \approx 66$ μm) to $\zeta = 450$ ($z \approx 120$ μm). The most effective focusing distance was $\zeta = 300$ ($z = 80$ μm). However, this value is very sensitive to changes in the laser pulse intensity and to the gas concentration and profile.

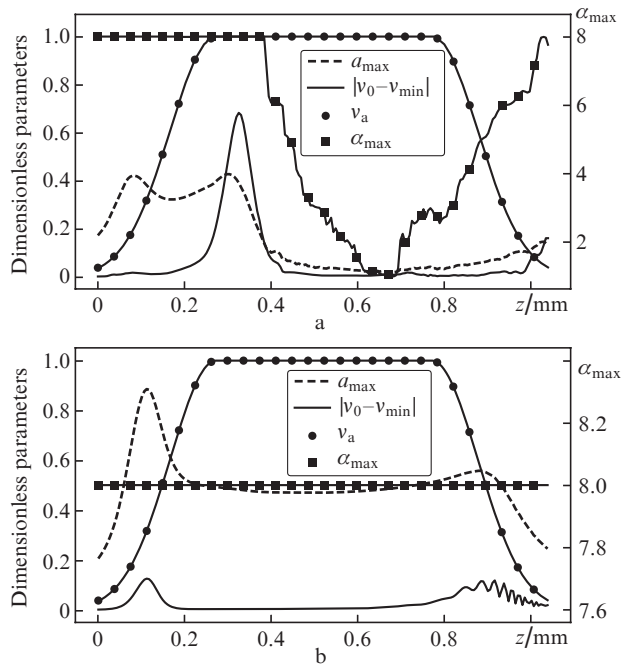

Figure 6. Distributions of the maximum dimensionless amplitude of the laser pulse field (a_{max}), the maximum amplitude of the wake wave ($|v_0 - v_{min}|$), the maximum degree of ionisation (α_{max}) and the normalised gas density (v_a) on the laser pulse propagation axis in the cases of (a) optical field ionisation (intensity of 0.7×10^{18} W cm^{-2}) and (b) a pre-ionised plasma (1.0×10^{18} W cm^{-2}) upon focusing of laser pulses at a distance $\zeta = 300$ ($z = 80$ μm).

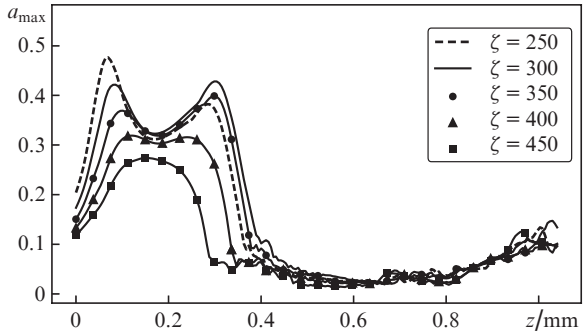

Figure 8. Distributions of the laser pulse amplitude a_{max} on the laser pulse propagation axis in the case of focusing to points at distances from $\zeta = 250$ ($z = 66$ μm) to $\zeta = 450$ ($z \approx 120$ μm).

5. Conclusions

We have analysed the spatial structure of wake fields and investigated the influence of optical field ionisation on their generation. In particular, we have found the possibility to generate wake waves in the case of optical field ionisation of gas for laser pulse parameters at which generation of wake waves in the case of a pre-ionised plasma is impossible (see Fig. 4). The consequence of this is a decrease in the threshold peak intensity of the laser pulse at which the wake of the plasma wave is generated in the case of optical gas ionisation. We have found that optical field ionisation leads to the formation of a sharp front of the laser pulse, which contributes to the appearance of the wake wave (see Fig. 4a).

On the other hand, in the case of optical field ionisation, there arises a restriction on the position of the focal plane of the laser pulse, which is associated with spatial inhomogeneity of the degree of optical field ionisation and ionisation refraction. With the used calculation parameters and focusing at distances greater than 0.08 mm from the beginning of the computational domain, the laser pulse cannot reach a critical intensity for the onset of self-modulation and self-focusing due to diffraction on the inhomogeneous electron density

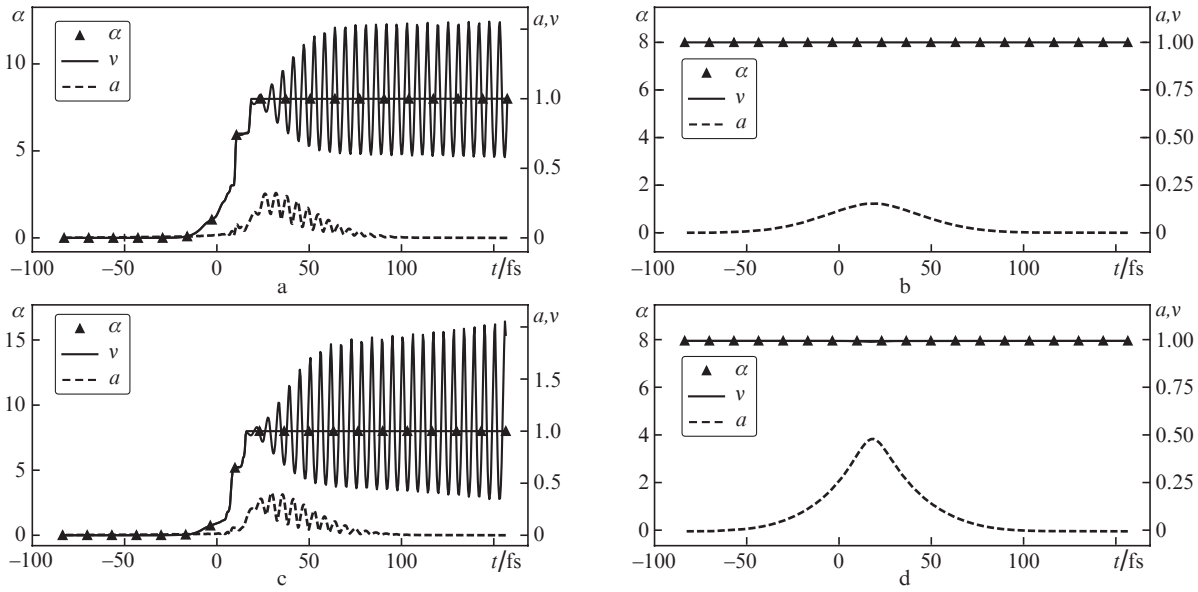

Figure 7. Comparison of the time dependences of the laser pulse envelopes (a), electron densities (v), and ionisation multiplicities (α) on the laser beam axis in the cases of (a) optical field ionisation [intensity of 1.3×10^{18} W cm^{-2}, focusing to the beginning of the computational domain ($\zeta = 0$)], (b) a pre-ionised plasma [intensity of 1.3×10^{18} W cm^{-2}, focusing to the beginning of the computational domain ($\zeta = 0$)], (c) optical field ionisation [intensity of 0.7×10^{18} W cm^{-2}, focusing at a distance $\zeta = 300$ ($z = 80$ μm)], and (d) a pre-ionised plasma [intensity of 1.0×10^{18} W cm^{-2}, focusing at a distance $\zeta = 300$ ($z = 80$ μm)] at point $\zeta = 1200$ ($z = 330.4$ μm).

profile resulting from optical field ionisation (Fig. 8). As a result, a wake wave is not generated.

Thus, the possibility of using a gas of atoms with a large number of electrons on the outer shell (argon, for example) to excite wake waves and accelerate electrons has been demonstrated. The main difference between this work and those performed earlier is the use of ionisation refraction to create conditions for the excitation of a wake wave in cases where, all other things being equal, its occurrence is impossible without optical field ionisation, while the laser pulse intensity is sufficient. To achieve maximum efficiency of the considered scheme, careful selection of the focusing position of the laser pulse is required. The possibility of electron acceleration in wake waves and their energy spectrum obtained in this way in the case of both external electron injection and trapping of background electrons (self-injection) requires further research.

Acknowledgements. This work was partially supported by the Presidium of the Russian Academy of Sciences under the Research Programme 'Extreme light fields and their interaction with matter', as well as by the Russian Foundation for Basic Research (Project No. 19-02-00908).

References

1. Gonsalves A.J., Nakamura K., Daniels J., Benedetti C., Pieronek C., de Raadt T.C.H., Steinke S., Bin J.H., Bulanov S.S., van Tilborg J., Geddes C.G.R., Schroeder C.B., Toth C., Esarey E., Swanson K., Fan-Chiang L., Bagdasarov G., Bobrova N., Gasilov V., Korn G., Sasorov P., Leemans W.P. *Phys. Rev. Lett*., **122**, 084801 (2019).
2. Emenko E.S., Kim A.V., Quiroga-Teixeiro M. *Phys. Plasmas*, **18**, 032107 (2011).
3. Andreev N.E., Veisman M.E., Cadjan M.G., Chegotov M.V. *Plasma Phys. Rep*., **26**, 947 (2000).
4. Andreev N.E., Chegotov M.V., Veisman M.E. *IEEE Trans. Plasma Sci*., **28**, 1193 (2000).
5. Andreev N.E., Gorbunov L.M., Kirsanov V.I., Pogasova A.A., Ramazashvili R.R. *JETP Lett*., **55**, 571 (1992) [*Pis'ma Zh. Eksp. Teor. Fiz*., **55**, 550 (1992)].
6. Leemans W.P., Clayton C.E., Mori W.B., Marsh K.A., Kaw P.K., Dyson A., Joshi C., Wallace J.M. *Phys. Rev. A*, **46**, 1091 (1992).
7. Andreev N.E., Chegotov M.V., Downer M.C., Gaul E.W., Matlis N.H., Pogosova A.A., Rundquist A.R. *IEEE Trans. Plasma Sci*., **28**, 1218 (2000).
8. Ho Y.-C., Hung T.-S., Yen C.-P., Chen S.-Y., Chu H.-H., Lin J.-Y., Wang J., Chou M.-C. *Phys. Plasmas*, **18**, 063102 (2011).
9. Goers A.J., Yoon S.J., Elle J.A., Hine G.A., Milchberg H.M. *Appl. Phys. Lett*., **104**, 214105 (2014).
10. Mora P., Antonsen T.M. *Phys. Plasmas*, **4**, 217 (1997).
11. Andreev N.E., Nishida Y., Yugami N. *Phys. Rev. E*, **65**, 056407 (2002).
12. Andreev N., Chizhonkov E., Frolov A., Gorbunov L. *Nucl. Instrum. Methods Phys. Res. A*, **410**, 469 (1998).
13. Ammosov M.V., Delone N.B., Krainov V.P. *Sov. J. Exp. Theor. Phys*., **64**, 1191 (1986) [*Zh. Eksp. Teor. Fiz*., **91**, 2008 (1986)].
14. Andreev N.E., Veisman M.E., Goreslavskii S.P., Chegotov M.V. *Plasma Phys. Rep*., **27**, 278 (2001).
15. Delone N.B., Krainov V.P. *Phys. Usp*., **41**, 469 (1998) [*Usp. Fiz. Nauk*, **168**, 531 (1998)].
16. Andreev N., Veysman M., Cadjan M., Chegotov M. *Plasma Phys. Rep*., **26**, 947 (2000).
17. Andreev N.E., Kuznetsov S.V. *IEEE Trans. Plasma Sci*., **36**, 1765 (2008).
18. Andreev N.E., Kuznetsov S.V. *Plasma Phys. Control. Fusion*, **45**, A39 (2003).